Performance Investigation of Modified Self- Commutated CSI-fed Induction Motor Drive

Pramod Agarwal [1] A.K. Pandey [2] V.K. Verma [1]

Abstract - The performance of modified self-commutating CSI-fed induction motor drive is investigated in this paper. The mathematical model of the complete drive system is developed in the synchronously rotating d-q reference frame to evaluate the performance of the drive. Closed form mathematical expressions are developed for the torque, phase voltage, efficiency, power factor, total loss etc. Performance of the drive is obtained experimentally and compared with the analytical results for validation

Keywords - Current Source Inverter, PWM Rectifier, Optimal Capacitor.

I. NOMENCLATURE

i_{as}, i_{bs}, i_{cs}	Line currents of the PWM inverter
v_s	Instantaneous stator phase voltage
i_c	Instantaneous phase current of capacitor
v_{ds}^e, i_{ds}^e	Voltage and current in d-axis stator winding in synchronous rotating reference frame
v_{qs}^e, i_{qs}^e	Voltage and current in q-axis stator winding in synchronous rotating reference frame
i_{dr}^e, i_{qr}^e	Current in d and q axes of the rotor winding in synchronous rotating reference frame
i_{cd}^e	Capacitor current in d axis winding in synchronously rotating reference frame
i_{cq}^e	Capacitor current in q axis winding in synchronously rotating reference frame
I_{act}	Active component of stator current
I_{react}	Reactive component of stator current
ω_e	Synchronous speed of the induction motor
ω_r	Rotor speed of induction motor
ω_{sl}	Slip speed of the induction motor
θ_e	Angular position of synchronous reference frame
I_{dc}	d.c. link current
t_e	Electromagnetic torque
t_l	Load torque
t_L	Rated load torque
V_{inv}	Input voltage of the inverter
I_{inv}	Input current of the inverter
V_r	Rectifier output voltage
r_f	Resistance of d.c. link inductor
l_f	Inductance of d.c. link inductor
l_{ss}, r_s	Self inductance and resistance of stator winding per phase
l_{rr} ,r_r	Self inductance and resistance of rotor winding per phase
l_m	Mutual inductance per phase
l_1	$l_s\ l_r - l_m^2$
C	Capacitance per phase
J	Moment of inertia in kg-m^2
B	Viscous friction coefficient
β	Pulse width of PWM rectifier
V_{LL}	Line to line input voltage of the rectifier
P	No. of poles

The paper first received 21 Feb. 2009 and in revised form 20 Aug 2009.
Digital Ref: A17050220

[1] Department of Electrical Engineering, Indian Institute of Roorkee, Roorkee, India
[2] Department of Electrical Engineering, Madan Mohan Malviya Engineering College, Gorakhpur, India

II. INTRODUCTION

The speed control of the induction motor is possible over a wide range by feeding the motor through a variable frequency Current Source Inverter (CSI). Due to controlled current operation of the inverter and thus inherent short circuit protection, slip regulated CSI is preferred over Voltage Source Inverter (VSI). The current source at the front end makes the system naturally capable of power regeneration without the need of extra converter as required in VSI. However, the line currents of conventional CSI-fed induction motor drive are non-sinusoidal in nature and have dominant low order harmonics. These lower order harmonics give rise to torque pulsation and hence, different PWM techniques in CSI are reported in

literature [1-5] which includes optimal PWM [2], speed pulsations. For the smooth speed control Programmed PWM [3] and Space Vector Modulation [5]. Another control technique to reduce the losses in the drives is presented in [6]. All these techniques are aimed to reduce the harmonics in the inverter output current but still the motor current is non-sinusoidal. To make the input power factor unity as well as motor current sinusoidal, techniques based on active filters are proposed in [11, 12]. The use of active power filter increases the cost and complexity.

In the present paper a modified self commutating CSI-fed induction motor drive is designed and developed so that the motor line voltages and currents are nearly sinusoidal over the wide range of the speed control. At the terminals of induction motor, a 3-phase capacitor bank is connected. The capacitor is designed such that it removes the harmonics from the machine currents over the wide operating frequency. The use of variable speed induction motor fed from variable frequency source for a particular application depends upon its steady state performance. The steady state analysis of the conventional current source induction motor drive has been reported in [7-10]. The aim of this paper is to investigate the steady state performance of the modified CSI drive. Simulation and experimental results are presented and compared to validate the mathematical model of the drive.

III. SYSTEM DESCRIPTION

The modified CSI fed induction motor drive consists of a three-phase ac source, PWM rectifier, dc link smoothening reactor, a current controlled inverter, a three-phase squirrel cage induction motor and three-phase

capacitor bank as shown in Fig 1. The input current source is realized using rectifier with current feed back. The output voltage of the rectifier is controlled using equal pulse width modulation technique. Thus the source current is having symmetrically placed equal width pulses which makes the input displacement factor unity and also reduces the harmonics injected into supply. The CSI output is controlled using space vector technique to reduce the harmonics in the output current. To operate the machine at a normal value of air gap flux, the motor is operated in statically unstable region of torque-slip characteristics using slip regulator in the feedback loop. The present work makes use of speed and current controllers of PI type. The actual speed of induction motor is measured by pulse encoder and compared with the reference speed set. The speed error is processed in the speed control loop to obtain the reference slip speed. Using slip regulator characteristics, the value of reference active stator current of the induction motor and reference reactive current are determined corresponding to reference slip speed.

The reference stator current is obtained using stator active reference current, the stator reactive reference current and the capacitor current as shown in the Fig.1. The stator current vs. slip speed and reactive stator current vs. slip speed characteristics together determine the slip regulator characteristics. These characteristics are shown in Fig.2 and Fig.3 and are obtained experimentally. The figures show that active current increases linearly with slip and hence with load while the reactive current is nearly constant all through out. Using reference active current, capacitor rms current and stator reference reactive current, stator reference current is determined, which is transformed to the dc link side to obtain the reference dc link current. The reference slip speed is added to the actual rotor speed to obtain the switching frequency of the inverter

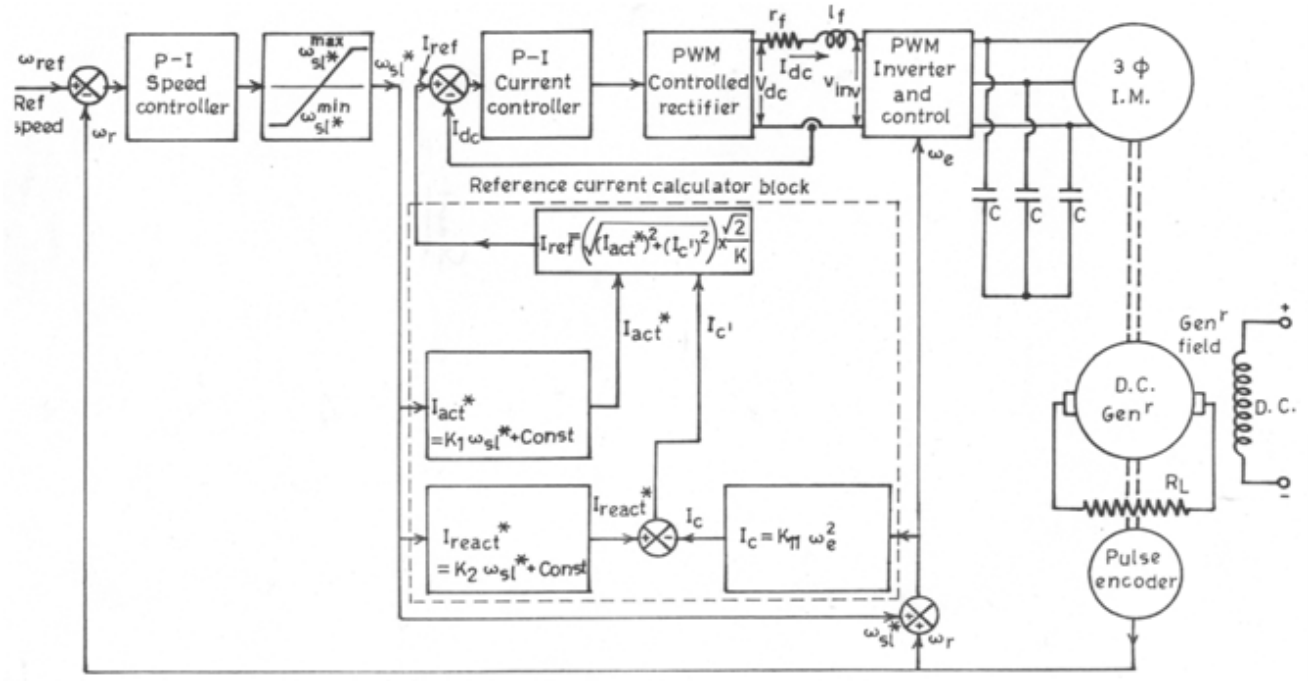

Fig 1: Variable speed modified current source inverter fed induction motor drive

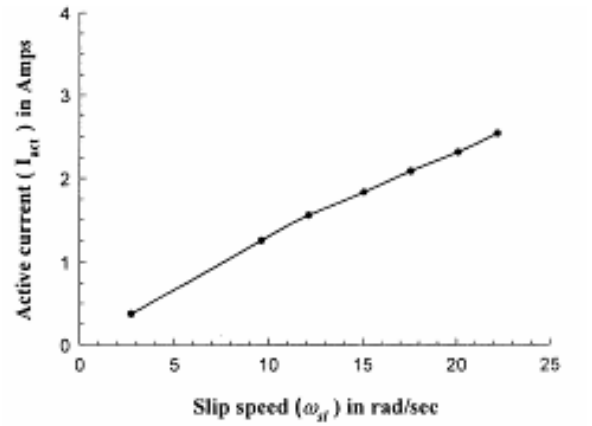

Fig 2: Active current vs slip speed characteristic

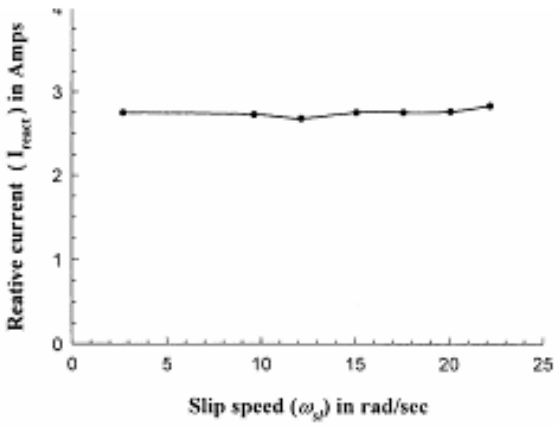

Fig.3: Reactive current vs slip speed characteristic

IV. MATHEMATICAL MODEL OF THE DRIVE

The modeling of the modified CSI fed induction motor drive is carried out in synchronously rotating reference frame.

Three-phase PWM Rectifier

The PWM rectifier output voltage depends upon the number of pulses per cycle and their widths. The converter is modeled for twelve numbers of equal pulses per cycle. It leads two pulses per 60°, each of β width. Fig.4 shows the output voltage waveform of PWM rectifier over a 60^0 interval.

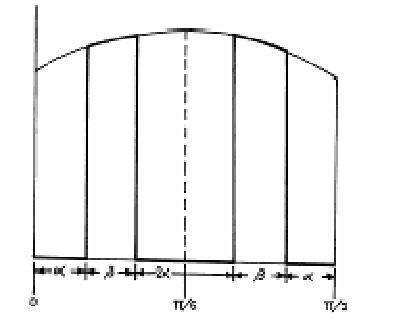

Fig 4: Output voltage of PWM Rectifier over 60^0

The average output voltage of the rectifier can beobtained in terms of pulse width β and can be expressed with the following expressions:

$$V_r = \frac{3\sqrt{2}}{\pi} V_{LL} \left(4 \sin \frac{5\pi}{12}\right) \sin \frac{\beta}{2} \quad (1)$$

Since β is varied from 10% to 90% of (π/6) radians, therefore,

$\sin(\beta/2) \cong (\beta/2)$ and

$$V_r = 5.218\, V_{LL}\, (\beta/2) \quad (2)$$

Three Phase Pulse Width Modulated Inverter

The output of CSI is controlled using space vector modulation. The fundamental component of line currents of the 3-phase pulse width modulated inverter i_{as}, i_{bs}, i_{cs} forms a balanced set of 3-phase currents with a maximum value as $I_{as(max)}$ and can be expressed as

$$I_{as(max)} = k\, I_{dc} \quad (3)$$

where, k is obtained with the help of Fourier analysis different PWM techniques in CSI are reported in of inverter line current waveforms. The value of k depends upon the operating frequency of the inverter and it varies from 0.8485 to 0.9970 for variation in operating frequencies from 10 Hz to 50 Hz. The q^e axis of the rotating reference frame is assumed to coincide with the stator a-axis at t = 0 as shown in Fig.5.

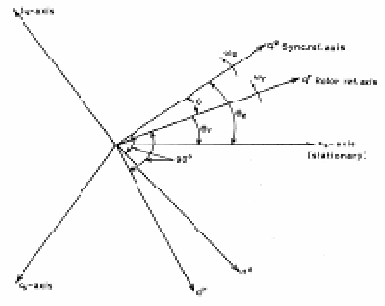

Fig.5: d-q reference frame

Since inverter output fundamental current peak is taken along the q^e axis of the reference frame, the transformed phase currents in the q^e-d^e reference frame are:

$$i_{0s}^{\ e} = 0;\ \ i_{qs}^{\ e} = k\, I_{dc};\ \ i_{ds}^{\ e} = 0 \quad (4)$$

Assuming power loss in the inverter to be negligible,
Inverter input power = Inverter output power

$$V_{inv} I_{inv} = v_{as} i_{as} + v_{bs} i_{bs} + v_{cs} i_{cs} = \frac{3}{2}\left(v_{qs}^{\ e} i_{qs}^{\ e} + v_{ds}^{\ e} i_{ds}^{\ e}\right) \quad (5)$$

Substituting the values of i_{qs}^e, i_{ds}^e and I_{inv} as I_{dc}, the inverter input voltage is obtained as:

$$V_{inv} = 1.5\, k\, v_{qs}^{\ e} \quad (6)$$

D C Link

The rectifier output voltage V_r is expressed as

$$V_r = 1.5\, k\, V_{qs}^{\ e} + \left(r_f + pL_f\right) I_{dc} \quad (7)$$

Three-phase Induction Motor

The induction motor can be modeled in q^e-d^e reference frame using the following assumptions.

- The three phase stator windings of the motor are balanced and sinusoidally distributed in space.
- The air gap flux is maintained at rated value.
- The motor line currents are sinusoidal due to capacitor at the motor terminals.
- The dc link current is ripple free.
- The switching transients in the inverter are ignored.
- There is no core loss in the induction machine.

The motor can be described by the following fourth-order matrix equation in q^e-d^e reference frame:

$$\begin{bmatrix} v_{qs}^e \\ v_{ds}^e \\ 0 \\ 0 \end{bmatrix} = \begin{bmatrix} r_s + pl_{ss} & \omega_e l_{ss} & pl_m & \omega_e l_m \\ -\omega_e l_{ss} & r_s + pl_{ss} & -\omega_e l_m & pl_m \\ pl_m & \omega_{sl} l_m & r_r + pl_{rr} & \omega_{sl} l_{rr} \\ -\omega_{sl} l_m & pl_m & -\omega_{sl} l_{rr} & r_r + pl_{rr} \end{bmatrix} \begin{bmatrix} i_{qs}^e \\ i_{ds}^e \\ i_{qr}^e \\ i_{dr}^e \end{bmatrix} \quad (8)$$

he electromagnetic torque equation of the motor is expressed as

$$t_e = \frac{3}{2} \cdot \frac{P}{2} \cdot L_m \left(i_{qs}^{\ e} i_{dr}^{\ e} - i_{qr}^{\ e} i_{ds}^{\ e}\right) \quad (9)$$

The equation of motion of the drive is expressed as

$$t_e = t_l + J \frac{d\omega_r}{dt} + B\, \omega_r \quad (10)$$

The load torque equation is given by:

$$t_l = t_L \cdot \left(\omega_r / \omega_{base}\right) \quad (11)$$

Three Phase Capacitor Bank

Assuming capacitor connected across the terminals of the stator to be loss less, the capacitor current is given as:

$$i_c = C \frac{dv_s}{dt} \quad (12)$$

Transforming the equation (12) in the synchronously rotating reference frame q^e-d^e ,

$$\left(\mathrm{i}^{\mathrm{e}}_{\mathrm{cd}}\ \cos\ \omega_{\mathrm{e}}\mathrm{t}\text{-}\mathrm{i}^{\mathrm{e}}_{\mathrm{cq}}\ \sin\omega_{\mathrm{e}}\mathrm{t}\right)=C\frac{d}{dt}\left(v^{e}_{ds}\cos\omega_e t-v^{e}_{qs}\ \sin\omega_e t\right)$$

$$\left.\begin{aligned}\mathrm{i}^{\mathrm{e}}_{\mathrm{cd}}\ &=\ \mathrm{C}\ (\mathrm{pv}^{\mathrm{e}}_{\mathrm{ds}}-\omega_e v^{e}_{qs})\\ \mathrm{i}^{\mathrm{e}}_{\mathrm{cq}}\ &=\ \mathrm{C}\ (\mathrm{pv}^{\mathrm{e}}_{\mathrm{qs}}+\omega_e v^{e}_{ds})\end{aligned}\right\}\qquad(13)$$

The equations (1) to (13) describe the mathematical model of the modified self-commutated CSI fed induction motor drive.

V. Steady State Analysis

The steady state performance of the drive is obtained using the mathematical model of the drive. The various steady state equations used in the performance analysis are given below:

$$V_{r(0)}=V_{inv(0)}+r_f\ I_{dc(0)}\qquad(14)$$

$$V_{inv(0)}=\frac{3}{2}\,\mathrm{k}\,v^{e}_{qs(0)}\qquad(15)$$

$$V_{r(0)}=1.5\,\mathrm{k}\,v^{e}_{qs(0)}+r_f I_{dc(0)}\qquad(16)$$

The steady state inverter current, machine current and capacitor current are related according to the following equations in q^e-d^e reference frame.

$$i^{e}_{invd(0)}=i^{e}_{dc(0)}+i^{e}_{ds(0)}\qquad(17)$$

$$i^{e}_{invq(0)}=i^{e}_{qc(0)}+i^{e}_{qs(0)}\qquad(18)$$

Since inverter output fundamental current peak is taken along the q^e-axis of the reference frame, therefore,

$$i^{e}_{invd(0)}=0\qquad(19)$$

$$i^{e}_{invq(0)}=\ \mathrm{k}\ I_{dc(0)}\qquad(20)$$

Capacitor current is expressed in q^e-d^e reference frame as given below:

$$i^{e}_{dc(0)}=\ -C\ \omega_e\ v^{e}_{qs(0)}\qquad(21)$$

$$i^{e}_{qc(0)}=C\omega_e\ v^{e}_{ds(0)}\qquad(22)$$

The steady state stator current equations in q^e-d^e reference frame are given by the following expressions.

$$i^{e}_{ds(0)}=\ C\ \omega_e\ v^{e}_{qs(0)}\qquad(23)$$

$$i^{e}_{qs(0)}=\ \mathrm{k}\ I_{dc}-C\omega_e\ v^{e}_{ds(0)}\qquad(24)$$

The steady state equation of the machine in q^e-d^e reference frame is as given below:

$$\begin{bmatrix}v^{e}_{qs(0)}\\ v^{e}_{ds(0)}\\ 0\\ 0\end{bmatrix}=\begin{bmatrix}\mathrm{r_s} & \omega_{\mathrm{e}}\mathrm{l_{ss}} & 0 & \omega_{\mathrm{e}}\mathrm{l_m}\\ -\omega_{\mathrm{e}}\mathrm{l_{ss}} & \mathrm{r_s} & -\omega_{\mathrm{e}}\mathrm{l_m} & 0\\ 0 & \omega_{\mathrm{sl}}\mathrm{l_m} & \mathrm{r_r} & \omega_{\mathrm{sl}}\mathrm{l_{rr}}\\ -\omega_{\mathrm{sl}}\mathrm{l_m} & 0 & -\omega_{\mathrm{sl}}\mathrm{l_{rr}} & \mathrm{r_r}\end{bmatrix}\begin{bmatrix}i^{e}_{qs(0)}\\ i^{e}_{ds(0)}\\ i^{e}_{qr(0)}\\ i^{e}_{dr(0)}\end{bmatrix}\qquad(25)$$

Under steady state condition, torque developed by the motor is equal to the load torque. Hence,

$$t_e=\frac{3}{2}.\frac{P}{2}.l_m\left(i^{e}_{qs(0)}\ i^{e}_{dr(0)}\right)=\ t_l\qquad(26)$$

Solving these equations, we can obtain the expressions for performance parameters of the drive.

VI. Selection Of Optimal Capacitor

To obtain the optimal value of capacitor required at the motor terminals for near sinusoidal current over a wide range of operating frequency, the steady state performance curves are plotted. These performance curves are obtained by computing the value of torque developed by the motor, power output, stator voltage per phase, stator current, power factor, power loss efficiency, dc link voltage for fixed value of dc link current, rated frequency and variable capacitance per phase and varying the slip from 0 to 1.

At the operating frequency and C=90μF/phase, slip-torque characteristic of Fig.6 shows that the torque developed by the machine is affected by the resonance. Therefore, higher value of capacitor is required. The performance curves are obtained for three different values of capacitor and are plotted against load torque as shown in Fig.6 to Fig.11. To explain these performance curves, the magnetization and rotor current variations with torque are also shown in Fig.12.

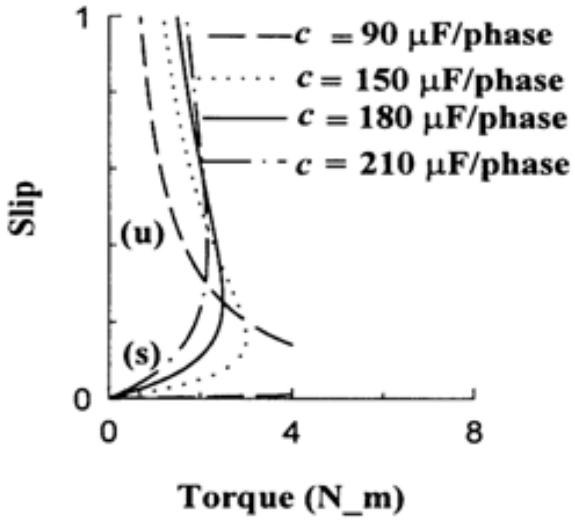

Fig.6: Variation of slip with load torque

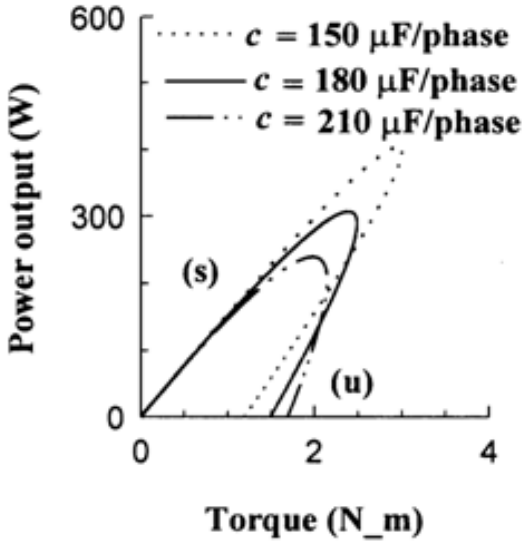

Fig.7: Variation of power output with load torque

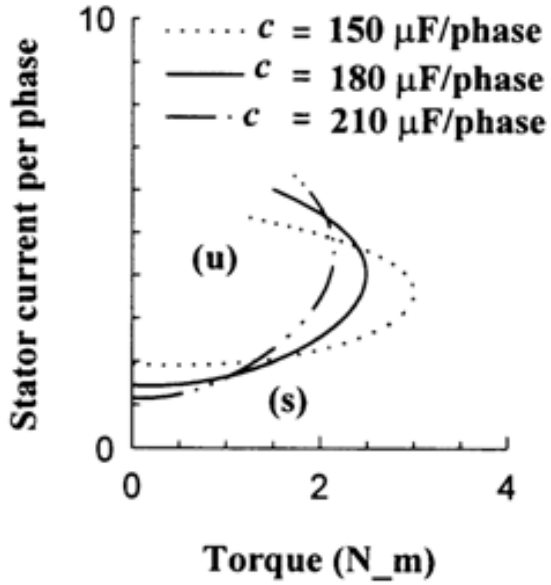

Fig.8: Variation of motor current with load torque

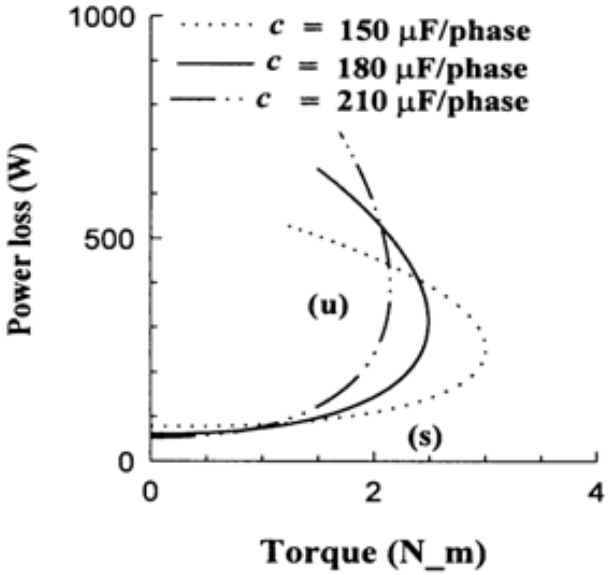

Fig.9: Variation of power loss with load torque

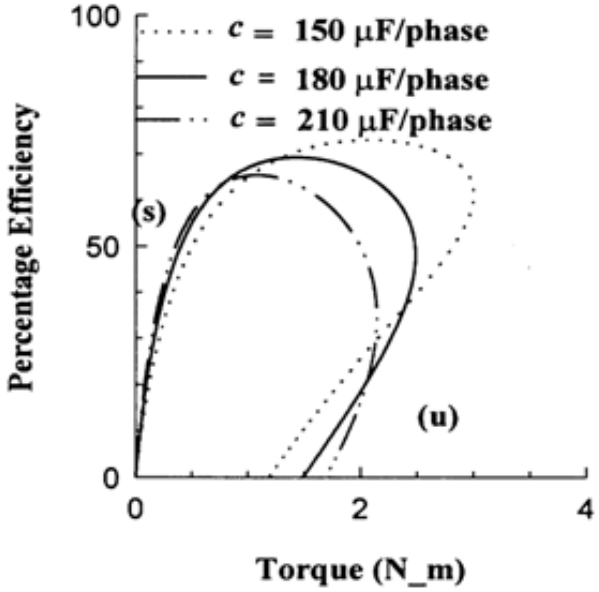

Fig.10: Variation of Efficiency with load torque

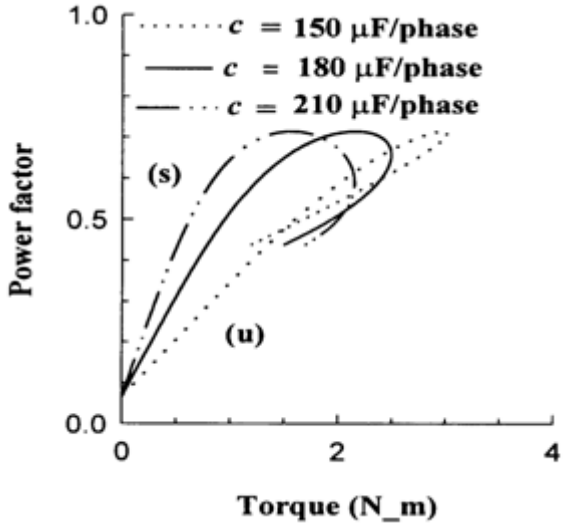

Fig.11: Variation of power factor with load torque

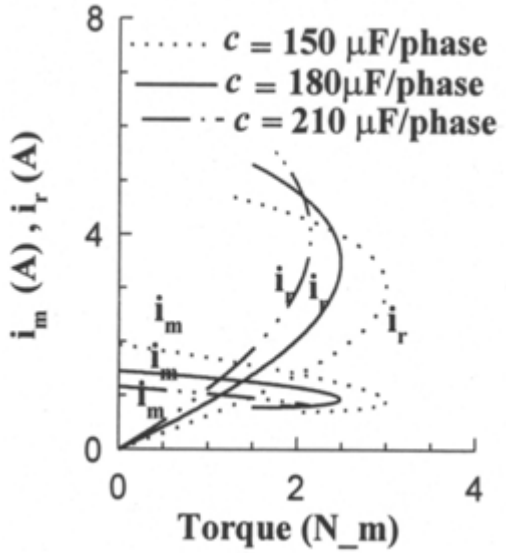

Fig.12: Variation of magnetizing and rotor current with load torque

Each curve is characterized by two regions, a stable region and an unstable region. In stable region as the capacitance increases, the slip increases for any value of torque. The peak value of torque decreases with the increase in capacitance while the slip corresponding to peak value of torque increases with the increase in capacitance. The starting torque is high at higher value of capacitance. Power output decreases with decrease in torque, in unstable region at each value of capacitance, because of low torque and high value of slip. The maximum value of power output reduces with the increase in capacitance. The stator current is the phasor sum of the magnetization and the rotor currents. As evident from the Fig.12, the magnetization current is nearly constant with respect to torque while the rotor current varies widely with torque. In the stable region at low value of slip, magnetization current is large in comparison to the rotor current, therefore stator current varies according to the variation in magnetization current. However, at high value of slip, rotor current is large in comparison to the magnetization current; therefore stator

current varies according to the variation of the rotor current. In the unstable region stator current increases with the decrease in torque corresponding to each value of capacitance because of high value of rotor current. The performance characteristics show that at a capacitor value of 150μF, the performance of the drive is better.

The experimental investigations are also carried out in open loop with the different values of capacitance across motor terminals, and it is found that the performance of the drive is found to be the best at this value of capacitor. Hence, 150μF value of capacitor is selected. The motor currents are recorded for different operating frequencies and are found to be close to sinusoidal. These currents are shown in fig.13 to fig.15.

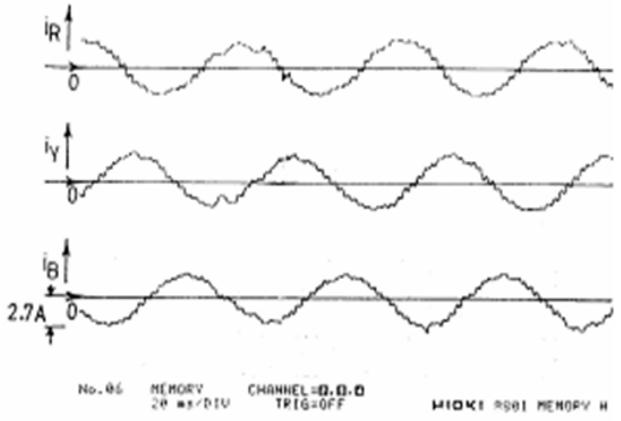

Fig.13: Motor line currents at 10 Hz operating frequency

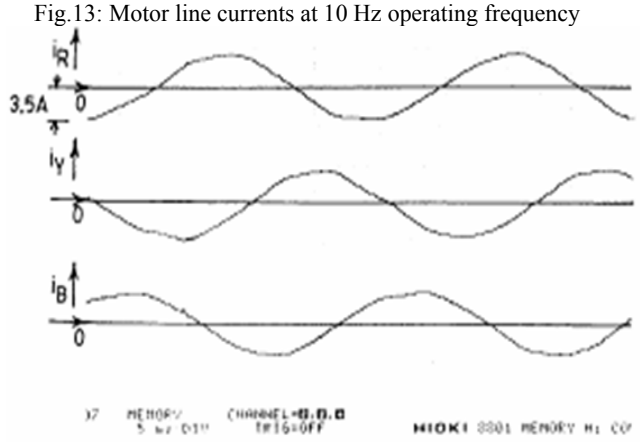

Fig.14: Motor line currents at 25 Hz operating frequen

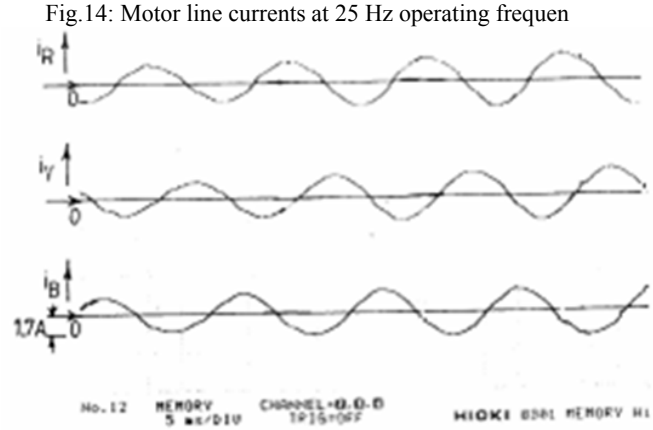

Fig.15: Motor line currents at 50 Hz operating frequency

VII. Results And Discussions

To investigate the performance of the drive, the machine is run at the rated frequency of 314rad/sec and current of 3.0 Amp and load test is performed. The drive performance parameters such as slip, power output, stator voltage, stator current, efficiency, output power factor, dc link voltage, input power factor are determined and plotted against developed torque.

To confirm the validity of the mathematical model of the drive, the performance of the drive is computed at the same operating conditions and plotted on the same graph. The experimental and analytical performance curves are shown in Fig.16 to Fig.23. The curves are in close conformity to each other.

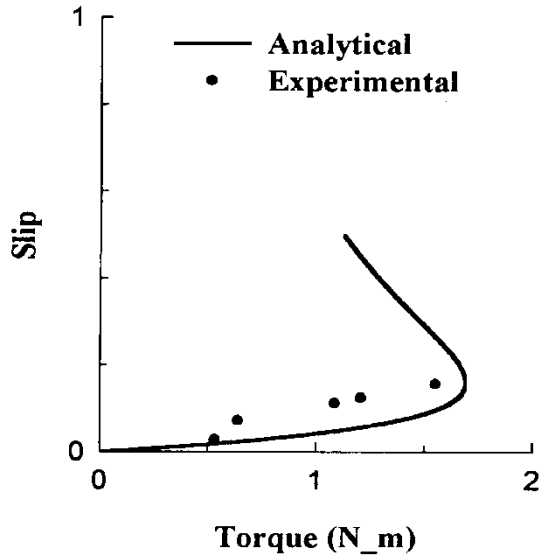

Fig.16: Slip vs torque characteristic

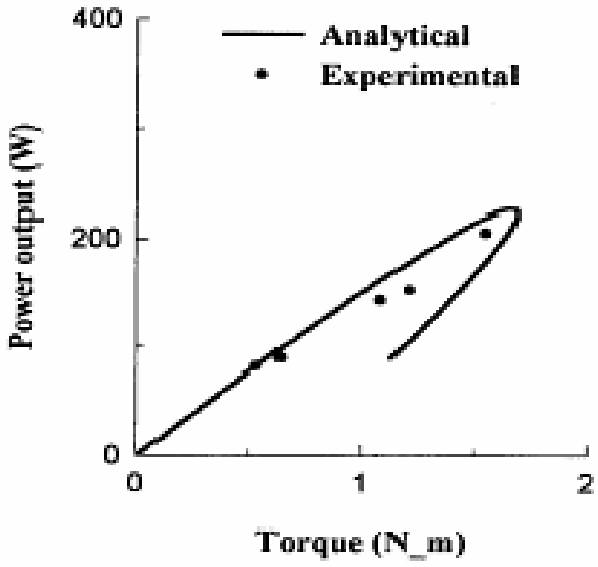

Fig.17: Power output vs torque characteristic

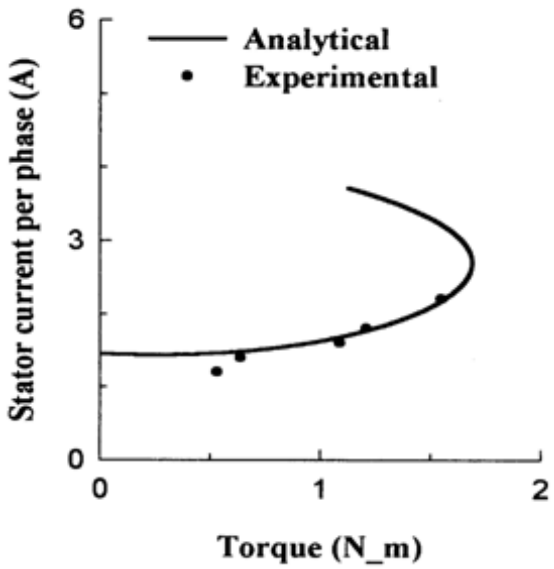

Fig. 18: Stator current vs torque characteristic

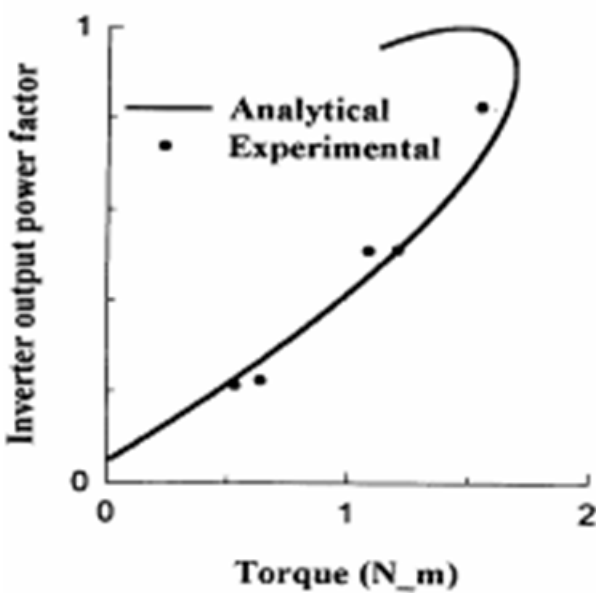

Fig. 21: Inverter output power factor vs torque characteristic

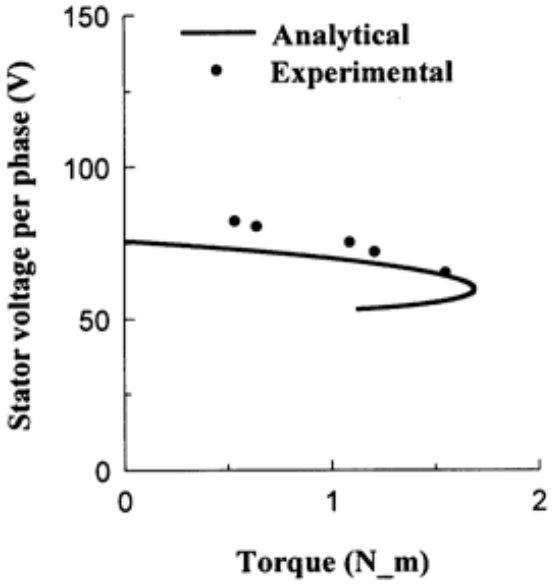

Fig.19: Stator voltage vs torque character

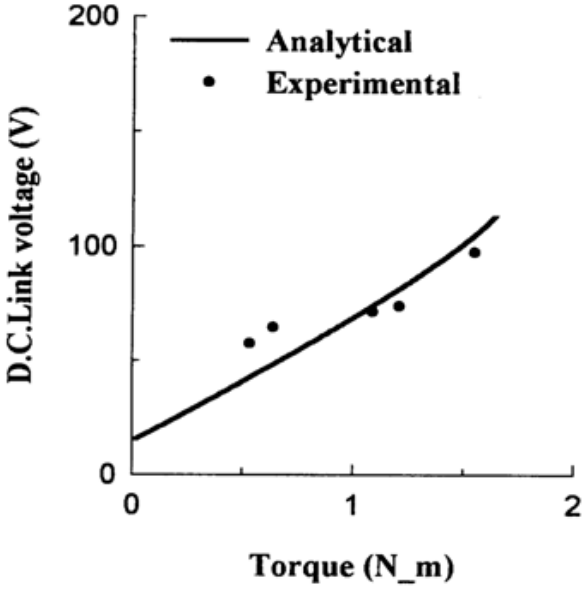

Fig.22: DC link voltage vs torque characteristic

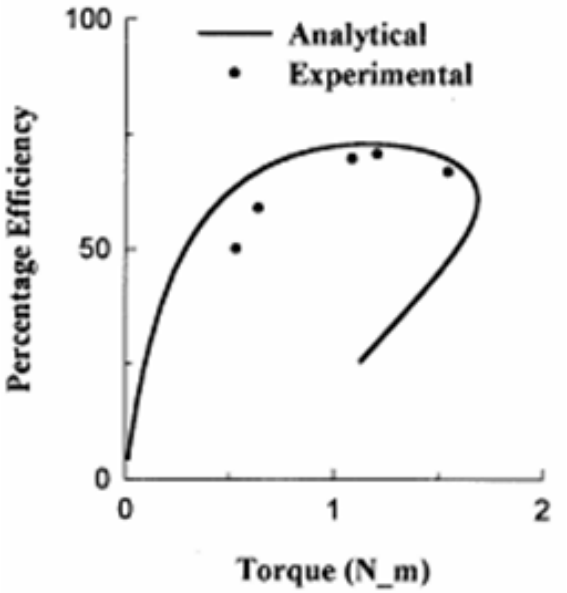

Fig.20: Efficiency vs torque characteristic

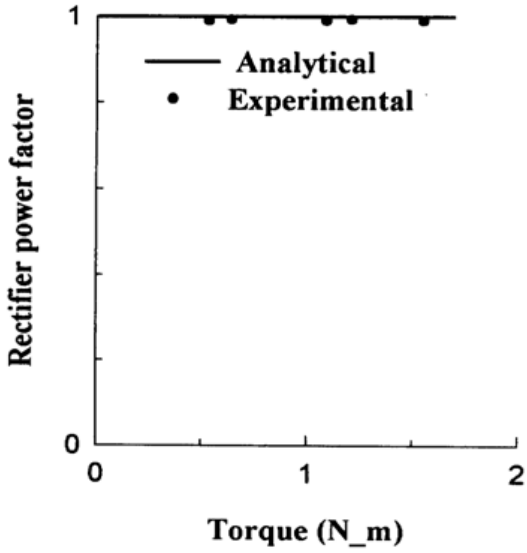

Fig.23: Input power factor vs torque characteristic

Slight deviation in the two curves is because of assumptions taken in the determination of analytical curves. For the same value of torque, slip obtained experimentally is more in comparison to the slip obtained analytically, since due to various power losses motor is not able to generate the same amount of torque at any speed as determined analytically. Therefore, the experimental power output at any value of torque is less in comparison to the power output obtained analytically. The power output increases with the increase in torque in both the cases. The stator current in both the cases are almost identical and very near to each other. The stator current variation with respect to torque is very small because with capacitance at the machine terminals. The magnetization and rotor currents are adjusted in such a manner that their phasor sum i.e. stator current varies very slowly with the torque. The efficiency increases with the increase in torque till maximum efficiency is achieved. At any value of torque experimentally obtained efficiency is less than the analytically obtained efficiency because of negligence of core, friction and windage losses. The power factor of the machine increases with the torque. Hence power factor of the inverter also increases with the increase in torque. For fixed value of dc link current the dc link voltage depends upon the input power demand of the machine. As the torque increases the power demand of the drive increases; hence dc link voltage increases with the torque. Both the power factors are quite close to each other at each value of operating frequency and torque. The analytically obtained power factor of pulse width modulated rectifier is always unity, while the experimentally obtained power factor is found to be very close to unity.

Thus, a good co-relation is found between analytical and experimental performance curves. The agreement between the analytical and experimental performance curves confirms the validity of the developed model considering various assumptions.

VIII. Conclusion

A modified self-commutating CSI-fed induction motor drive is presented. The steady state performance expressions are developed. The steady state performance of the drive is drawn at the different value of capacitances to select the capacitor required at the machine terminals. The optimal value of capacitor is selected from the curves for high power output, acceptable current, minimum power loss and maximum efficiency. The steady state performance curves at the optimum value of capacitance are drawn through simulation and are compared with the experimental curves drawn at the rated operating frequency and fixed dc link current in the open loop.

Appendix

Induction Motor Parameters
3-phase, 400V, 50 Hz, star connected, 1.0 H.P.
$r_s = 3.52\ \Omega$, $r_r = 2.78\ \Omega$, $l_{ss} = 0.165$ H
$l_{rr} = 0.165$ H, $l_m = 0.15$ H, $J = 0.01289$ kg-m^2

D.C. Link Parameters
$r_f = 0.250\ \Omega$, $L_f = 0.04$ H

References

[1] S. Nonka and Y. Neba, "New GTO current source inverter with pulse width modulation control techniques", IEEE Transactions on Industry Applications, Vol. IA-22, No. 4, July/Aug 1986, pp. 666-672.

[2] S.R. Bowes and R.I. Bullough, "Optimal PWM microprocessor controlled current-source inverter drives", IEEE proceedings, Vol. 135, Pt. B, No. 2, March 1988, pp. 59-75.

[3] P..N. Enjeti, P.D. Ziogas and J.F. Lindsay, "Programmed PWM technique to eliminate harmonics: A critical evaluation", IEEE Transactions on Industry Applications, Vol. 26, No. 2, March/April 1990, pp. 302-315.

[4] N.R. Zargari, Y. Xiao and Bin Wu, "Near unity input displacement factor for current source PWM drives", IEEE Industry Applications Magazine, July/Aug. 1999 pp. 19-25.

[5] S.R. Bowes and S. Grewal, "Novel harmonic elimination PWM control strategies for three phase PWM inverters using space vectors techniques", IEEE Proceedings Electric Power Applications, Vol. 146, Sept. 1999, pp. 495-514.

[6] J.R. Espinoza and G. Joss, "A current-source inverter-fed induction motor drive system with reduced losses", IEEE Transactions on Industrial Applications, Vol.34, No. 4, pp. 796-805.

[7] N. Sawaki and N.Sato, "Steady-state and stability analysis of induction motor driven by current source inverter", IEEE Transactions on Industry Applications, Vol. IA-13, No. 3, May/June 1977pp. 244-251.

[8] E.P. Cornell, and T.A. Lipo, "Modeling and design of controlled current induction motor drive system", IEEE Transactions on Industry Applications, Vol. 13, July/Aug. 1977,pp. 321-329.

[9] A. Joshi and S.B. Dewan, "Modified steady-state analysis of the current-source inverter and squirrel cage motor drive", IEEE Transactions on Industry Applications, Vol. IA-17, No. 1, Jan/Feb 1981, pp. 50-57.

[10] P. Agarwal and V.K. Verma, "Performance evaluation of current source inverter- fed induction motor drive", Journals of Institution of Engineers, Vol.72, February 1992, pp. 209-217.

[11] S. Kwak and H.A. Toliyat, "A hybrid solution for load commutated inverter fed induction motor drive", IEEE Transactions on Power Electronics, Vol.41, No.1, Jan/Feb 2005, pp.83-90.

[12] Abdul Rahiman Beig and V.T. Ranganathan, "A novel current source inverter fed induction motor drive", IEEE Transactions on Power Electronics, Vol.21, No.4, July 2006, pp-1073-1082.

Biographies

Pramod Agarwal (M'99) received the B.E., M.E., and Ph.D degrees in Electrical Engineering from the University of Roorkee, India, in 1983, 1985 and 1995, respectively.

He joined the erstwhile University of Roorkee, India in 1985 as Lecturer. He was a Postdoctoral Fellow with the Ecole de technologie superior, University of Quebec, Montreal, Canada. He is currently a Professor with the Department of Electrical Engineering, Indian Institute of Technology, Roorkee, India. He has developed a number of educational units for laboratory

experimentation. His fields of specialization are electrical machines, power electronics, microprocessor and microcomputer controlled ac/dc drives, active power filters, multi-level inverters and high power factor converters.

Ashok Kumar Pandey born in 1964, did B.E. (Electrical) from M. M .M. Engineering College, Gorakhpur, India in 1987, M.Tech. (Power Electronics, Electrical Machines and Drives) from Indian Institute of Technology, Delhi in 1995 and Ph.D. from Indian Institute of Technology, Roorkee in 2003.
He joined the Electrical Engineering Department, M. M. M. Engineering College, Gorakhpur, India in 1987 and is presently working as an Assistant Professor. His area of interest includes Power Electronics, Electrical Machines and Drive

V.K. Verma did B.E. (Electrical Engineering) from Government Engineering College, Jabalpur in 1962 and M.E. and Ph.D. from University of Roorkee, Roorlee, India in 1965 and 1976 respectively. He joined Electrical Engineering Department at University of Roorkee, India in 1969 as Reader and became Professor in 1978.
He retired in the year 2000 from University of Roorkee and is currently a Professor with the Department of Electrical Engineering, College of Engineering, Roorkee. India. His field of research work is Power Apparatus and Electric Drives and microprocessor applications